



Examining injection properties of boreal forest fires using surface and satellite measurements of CO transport

Edward J. Hyer,^{1,2} Dale J. Allen,³ and Eric S. Kasischke¹

Received 8 November 2006; revised 11 June 2007; accepted 20 June 2007; published 25 September 2007.

[1] Boreal forest fires are highly variable in space and time and also have variable vertical injection properties. We compared a University of Maryland Chemistry and Transport Model (UMD-CTM) simulation of boreal forest fire CO in the summer of 2000 to surface observations from the NOAA Cooperative Air Sampling Network and satellite observations of CO from the Measurement of Pollutants in the Troposphere (MOPITT) instrument to investigate the sensitivity of these measurements to injection height and to evaluate the bulk injection properties of the boreal fire source. Our results show that emissions at the surface produce more than twice the signal in surface CO measurements compared with emissions injected into the upper troposphere. Surface injection yielded the best agreement with surface observations, but high-altitude injection resulted in very small variations at the surface, and so the statistical comparison with surface observations was inconclusive. Because of the vertical sensitivity of MOPITT, estimated total CO burden north of 30°N was 10% higher for upper tropospheric injection of boreal forest fire CO compared to surface release. We used a contrast filter to select the MOPITT retrievals most sensitive to boreal forest fire injection height and found that the best agreement between simulation results and MOPITT observations was obtained with midtropospheric injection of emissions and with pressure-weighted distribution of emissions through the tropospheric column. Appendix A uses CTM output to examine quantitatively the bias and errors in calculations of total column CO and total CO burden using MOPITT CO retrievals.

Citation: Hyer, E. J., D. J. Allen, and E. S. Kasischke (2007), Examining injection properties of boreal forest fires using surface and satellite measurements of CO transport, *J. Geophys. Res.*, 112, D18307, doi:10.1029/2006JD008232.

1. Introduction

[2] Emissions from boreal forest fires contribute significantly to the atmospheric composition of the Northern Hemisphere, and are extremely variable on both seasonal and interannual scales [Dlugokencky *et al.*, 2001; Kasischke *et al.*, 2005; Novelli *et al.*, 2003; Yurganov *et al.*, 2004]. Improved atmospheric measurements have shown potential for improving constraints on terrestrial sources of trace gases using inverse modeling of atmospheric transport and chemistry [Gerbig *et al.*, 2003; Gurney *et al.*, 2002]. Modeling the atmospheric effects of boreal forest fires requires a spatially and temporally resolved estimate of the source, which can show very different spatial and temporal patterns from year to year [Kasischke *et al.*, 2005; Murphy *et al.*, 2000; Stocks *et al.*, 2003]. Recent

modeling efforts have begun to include high-resolution estimates of biomass burning activity to estimate its effects on the global atmosphere (e.g., Hoelzemann *et al.* [2004], van der Werf *et al.* [2003], and van der Werf *et al.* [2006], as well as numerous studies at regional scales). In addition to their horizontal and temporal variability, boreal and temperate forest fires also show a wide range of variation in the vertical distribution of emissions at the source, commonly referred to as the injection height. Studies of specific cases have found that smoke plumes from individual fires are sometimes almost entirely confined within the planetary boundary layer (PBL) [e.g., Trentmann *et al.*, 2002], and sometimes extend up beyond the tropopause, introducing trace gases and aerosols into the stratosphere [e.g., Fromm *et al.*, 2000]. There is also evidence that injection height has significant variability in some tropical fires as well [see, e.g., Freitas *et al.*, 2006].

[3] This study uses a chemistry and transport model (CTM) simulation of boreal fire activity during the summer of 2000 to examine the implications of injection height for inverse modeling of the boreal fire source. Rather than model the plume characteristics of individual fires, model scenarios are chosen to represent the range of injection conditions, in order to study the bulk properties of the boreal fire CO source. Results obtained under specific injection conditions are compared to atmospheric CO observations from the

¹Department of Geography, University of Maryland, College Park, Maryland, USA.

²Now at Naval Research Laboratory, Marine Meteorology Division, Monterey, California, USA.

³Department of Atmospheric and Oceanic Sciences, University of Maryland, College Park, Maryland, USA.

NOAA Cooperative Air Sampling Network (CASN) as well as CO retrievals from the MOPITT instrument. Specific goals of this study are (1) Describe the interaction between injection height and the signal of boreal forest fire CO in surface and satellite measurements. (2) Examine the implications of this interaction for inverse modeling of CO sources. (3) Characterize the bulk injection properties of the boreal fire CO source by comparison of simulation results to observations.

[4] This study uses similar methodology to recent work by *Leung et al.* [2007]. While the atmospheric model, atmospheric observations, and modeling assumptions differ, the two studies use the same surface observations, as well as similarly derived estimates of the boreal fire CO source. The results of that study make a valuable point of reference for this one, and are dealt with in detail in the discussion sections of this paper.

[5] The remainder of the introduction will present a brief overview of theoretical, observational, and modeling work on injection height. Section 2 describes the transport and chemistry simulation experiment, the atmospheric data used, and gives some detail on the specific methods used to compare model output to observations. Section 3 is divided into two parts. The first part presents results of the simulation showing how injection height affects the observed magnitude of the CO source from boreal forest fires. The second part compares model outputs to atmospheric observations. Conclusions are presented in section 4. Appendix A describes quantitatively the effects of the transformation of CTM model output to match the sampling properties of MOPITT CO retrievals.

1.1. Theory of Forest Fire Smoke Injection

[6] Trace gas emissions from surface sources generally enter the atmosphere near the ground with low surplus energy. These emissions are rapidly cooled to the background air temperature, mixed through the boundary layer, and mixed into the free troposphere by turbulent mixing and convection as determined by local meteorological conditions. However, there is abundant evidence that forest fire emissions are often lofted into the free troposphere by a process both faster and more coherent than turbulent mixing. Emissions lofted in this fashion will enter the free troposphere with far less dilution and less chemical and physical alteration compared with emissions entrained from the boundary layer under ordinary meteorological conditions [*Goode et al.*, 2000; *Hobbs et al.*, 1996]. This high-energy convective lofting alters the vertical profile of emissions over the geographic source, and produces transport outcomes similar to having an emissions source located in the free troposphere. Accurate simulation of the transport pathways and chemical evolution of forest fire emissions requires that the vertical distribution of emissions be correctly described.

[7] Injection of forest fire smoke is governed by both the energy of the fire and the stability of the local atmosphere. The energy transfer from the advancing front of a forest fire can be estimated by the fire intensity $I = cmr$, where c is the heat of combustion of the fuel, m is the mass of fuel consumed, and r is the rate of fire spread [*Byram*, 1959]. The output from this calculation is kilowatts of energy per meter of the flaming front. For large forest fires, this

value can exceed $50,000 \text{ kW m}^{-1}$ [*Stocks and Kauffman*, 1997], which is sufficient to cause convective lofting of fire smoke above the PBL independent of local stability conditions. When this lofting occurs, fires are said to be “plume-dominated,” indicating that the vertical mixing is dominated by the buoyancy of the hot fire emissions. *Fromm and Servranckx* [2003] propose a positive feedback in these cases whereby a hot emissions plume lofting upward through an unstable atmosphere might strengthen the instability, resulting in stronger winds at the surface as well as enhanced lightning. This would both create conditions favorable to further burning and enhance convective lofting of emissions. Effects of this type are the reason that plume-dominated fires are said to “create their own weather.” Fire-related meteorological phenomena are colloquially referred to as “firestorms”; for two different modeling approaches to analyzing these phenomena, see *Nelson* [2003] and *Trentmann et al.* [2006].

[8] *Lavoue et al.* [2000] derived values for I from several experimental fires, and proposed a linear relation between I and injection height. While this proposed relationship was based on very sparse data, it did highlight the significant energy difference between crown and surface fires, as well as the higher energy associated with larger fires. *Lavoue et al.*'s [2000] empirical relationship between I and injection height implies that the range of burning conditions commonly observed in the boreal zone could result in effective injection heights ranging from 2500 m for surface fires to above 7500 m for large crown fires. However, local meteorological conditions can suppress or promote lofting, resulting in a broader range of outcomes. This theoretical range of effective injection heights has been verified by studies of wild and experimental fires, as discussed below.

1.2. Direct Evidence for Forest Fire Injection Height

[9] Direct observations of emissions plumes from wild-fires and experimental forest fires demonstrate the range of effective emission heights. They do not provide a generalized picture of the properties of the boreal forest fire source, but are illustrative of the range of source behavior.

[10] *Fromm and Servranckx* [2003] performed a detailed satellite analysis of a large forest fire in NW Canada, using satellite measurements to identify smoke-polluted air masses and calculate height and temperature of the plume top. The case that they examined, in May 2001, combined energetic burning with extremely active convection to loft smoke emissions up to the tropopause, where a small fraction of the plume entered into the stratosphere. *Jost et al.* [2004] analyzed observations from aircraft measurements off the coast of Florida, and found enhanced aerosol and CO in the middle stratosphere between 14.7 and 15.8 km above sea level. These enhancements were shown by trajectory calculations and satellite data analysis to have originated from fire activity in Saskatchewan. This type of extreme event appears to be uncommon: *Livesey et al.* [2004] examined more than a decade of satellite data from the Microwave Limb Sounder, and found only one episode of forest fire smoke intrusion into the midstratosphere. Further research is needed to better understand the frequency and effects of stratospheric injection of forest fire emissions.

[11] *Goode et al.* [2000] flew aircraft over active wildfires in Alaska, and report plume heights in the range of 1500–2500 m for fires in forested areas. They sampled a range of fire sizes and fuel densities. The observations they made give a reasonable idea of how injection might function in a high fire danger condition, but the sample is too small to indicate the distribution of conditions or the frequency of outliers.

[12] Detailed observations were made of the smoke plume from the Smoke, Clouds and Radiation-C (SCAR-C) experimental fire in the Pacific Northwest [*Hobbs et al.*, 1996]. This was a small prescribed fire of logging debris. Measurements of the smoke plume from this fire showed that in the center of the fire, smoke was lofted to 600 m, while smoke outside the hottest part of the fire was held below 300 m by a strong inversion [*Trentmann et al.*, 2002].

[13] These observations are indicative of the range of injection conditions for temperate and boreal forest fires. Process-based modeling of the complex interaction between fire energy and local meteorology requires data that are not systematically available for regional-scale experiments. Modeling experiments simulating atmospheric transport of fire emissions have relied on simple parameterizations of the injection process, and the results of these experiments shed some light on the injection process.

1.3. Treatment of Smoke Injection in Transport-Modeling Experiments

[14] *Forster et al.* [2001] modeled the transport of emissions from North America to Europe in August 1998. They concluded that large forest fires in northwest Canada were responsible for aerosol enhancements observed over the European continent as well as enhanced CO measured at Mace Head, Ireland. Their transport simulations distributed the forest fire emissions evenly between the surface and 2500 m at the source. Another study of the same fire events, however, used an injection height range of 3000–5000 m to produce the best match with observations of NO₂ from the Global Ozone Monitoring Experiment (GOME) and the TOMS aerosol index [*Spichtinger et al.*, 2001].

[15] In some cases, local instability may accomplish the same effect as convective lifting caused by energetic burning. *Lamarque et al.* [2003] modeled the CO emissions from a group of fires in the northwestern United States in 2000, using the MOZART-2 chemical transport model. They released the forest fire CO at the surface, and found it was immediately lofted into the midtroposphere. *Colarco et al.* [2004] modeled a plume from forest fires in Quebec in July 2002, examining which injection scenarios most effectively reproduced measurements taken over Washington, DC. They found that good results could be obtained by releasing the emissions at the surface, where local convection would immediately lift them into the free troposphere, or by releasing emissions at altitude. However, they found that the approach of distributing the initial emissions release in the lower troposphere above the boundary layer (500–~3000 m) produced results inconsistent with their observations, because the bulk of the emissions subsided rapidly to the surface and did not arrive at the measurement location.

[16] *Leung et al.* [2007] used the GEOS-CHEM global chemistry and transport model to compare transport simulations of boreal forest fire smoke using three different

injection scenarios (surface injection, mixing through the troposphere, and a 60:40 split of emissions above and within the boundary layer). They found that surface and total column CO measurements respond very differently to sources with different injection heights, and that minimization of error to optimize injection height and source magnitude gives different results with the two types of observations. The experiments in this paper are complementary to this work, examining in more detail the response of atmospheric observations to injection properties of CO sources.

[17] *Freitas et al.* [2006] used a 1-D model of plume rise to describe injection of fire emissions in a coarse resolution 3-D transport model. Their model of pollution transport over South America identified several cases where plumes from vigorous fires were in better agreement with observations when injection into the midtroposphere was included. They also found that simulations without the plume rise model consistently overestimated CO concentration in the boundary layer.

[18] Effective injection height of emissions over a fire event is the result of both the energy of the fire itself and the local meteorological conditions. Physical modeling of injection requires an accurate estimate of the energy release from a fire [*Lavoue et al.*, 2000], which requires data about fuel properties and fire conditions which are difficult to obtain at regional and global scales. Because of this difficulty, plume rise models such as the one described in *Freitas et al.* have not yet been implemented in global models.

[19] The purpose of this study is to describe the bulk vertical properties of CO from boreal forest fires by evaluating simulations of the range of tropospheric injection scenarios. The simulations in this study use simple uniform assumptions to investigate the atmospheric effects of a range of smoke injection scenarios. The bulk properties of the CO source will be useful for tuning a plume rise model for implementation in a global model.

2. Methods

2.1. Overview

[20] CO emissions from boreal forest fires were simulated for the 2000 fire season using the Boreal Wildfire Emissions Model (BWEM) [*Kasischke et al.*, 2005]. These emissions were used as input to a transport and chemistry simulation run with the University of Maryland Chemistry and Transport Model (UMD-CTM). Simulation results were compared with surface CO observations from the NOAA Cooperative Air Sampling Network (CASN) and satellite observations from the Measurement of Pollution in the Troposphere (MOPITT) instrument. Simulation results and observations were compared for the period 1 June to 31 August.

2.2. Boreal Forest Fire CO Emissions

[21] CO emissions from boreal forest fires were estimated using the data inputs described by *Kasischke et al.* [2005]. The source estimate used here uses differs from the estimate published by *Kasischke et al.* [2005] in the following ways:

[22] 1. CO emissions from Russian fires are calculated on the basis of an estimated fraction of biomass consumed in aboveground and ground layer fuels, similar to the approach

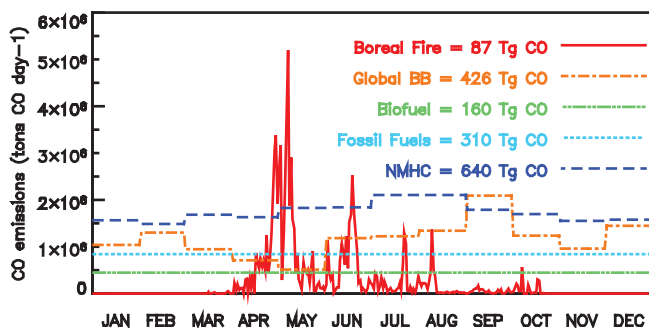


Figure 1. Time series of surface CO sources for the year 2000 used in the simulations for this study. Details of sources are given in section 2.3. The “Global Biomass Burning” source is the Global Fire Emissions Database version 1.0 [van der Werf et al., 2003] with boreal regions excluded.

used by French et al. [2000]. This results in CO emissions much higher than those of the “moderate” scenario given by Kasischke et al. [2005], which uses a depth-of-burn model to estimate fuel consumption in the ground layer.

[23] 2. North American CO emissions are estimated using regionally averaged levels of fuel consumption, following the method of Amiro et al. [2001], instead of the spatially resolved approach used by Kasischke et al. [2005]. This difference did not significantly affect total CO emissions.

[24] 3. The estimate used here does not include a seasonal parameterization of fire severity. This results in total carbon and trace gas emissions higher than those of Kasischke et al. [2005], especially for May fires.

[25] The year 2000 was a moderate to large fire year compared with other recent years in Russia, and a low fire year in Canada and Alaska, compared to both recent and long-term inventories [Stocks et al., 2003; Sukhinin et al., 2004]. With the parameters used for this study, boreal fires in 2000 produced an estimated total of 87.6 Tg CO (compare to 44.5 Tg, the “moderate” scenario given by Kasischke et al. [2005]). Comparisons of emissions models for boreal fires [Leung et al., 2007; Soja et al., 2004; Yurganov et al., 2004] have shown that the Kasischke et al. [2005] model is at the high end of estimates, so the calculations used for this study should be considered a likely overestimate of boreal forest fire CO.

[26] Of the total boreal fire CO emissions, 83.5 Tg was from 9.3 Mha of fire in Russia, of which 63% occurred before 1 June. The remaining CO was from fires during June–August in Canada and Alaska. Russian fires in May were the largest events in the boreal zone during 2000, but May observations were not included in this study because of Mongolian steppe fires near the Russian boreal zone that produced excessive interference in the signal from boreal fires.

2.3. Other CO Sources

[27] Figure 1 shows the annual time series of all surface CO sources used in this study. All the principal sources of CO to the atmosphere were included in the CTM simulation, with the exception of CO from soils, which

are expected to be a minor contributor to overall CO emissions, and for which no comprehensive data source is available [Kuhlbusch et al., 1998; Zepp et al., 1997]. Fossil fuel CO (Figure 1 “Fossil Fuels”) was estimated with the inventory described by Bey et al. [2001], with Asian emissions from the inventory of Streets et al. [2003] superimposed. CO emissions from biomass burning outside the boreal zone were taken from the Global Fire Emissions Database product, version 1.0 (Figure 1 “Global BB”) [van der Werf et al., 2003]. This database estimates emissions using fire size, location, and timing inputs from the Tropical Rainfall Monitoring Mission (TRMM) and Along Track Scanning Radiometer (ATSR) satellite instruments [Giglio et al., 2003; van der Werf et al., 2004], and estimates fuel consumption using a dynamic vegetation model, the Carnegie-Ames-Stanford Approach (CASA) [Potter et al., 1993]. Production of CO from biofuel combustion including agricultural burning and fuelwood use (Figure 1 “Biofuel”) was estimated on the basis of the inventory of Yevich and Logan [2003]. All of these surface sources were released into the lowest layer of the CTM.

[28] In addition to surface sources, the model includes photochemical production of CO from methane oxidation as well as isoprene and terpene oxidation. Methane oxidation was calculated online using fixed methane fields from Dlugokencky et al. [1994] scaled to the year 2000 and OH fields from Spivakovsky et al. [2000]. Production of CO from oxidation of isoprene and terpene (Figure 1 “NMHC”) was calculated offline using the method of Allen et al. [1996a].

[29] The principal atmospheric sink of CO is oxidation by hydroxyl, and this mechanism is calculated online in the CTM. Fixed OH fields from Spivakovsky et al. [2000] were used.

2.4. Transport Simulation

[30] Transport and chemistry of CO were simulated with the University of Maryland CTM (UMD-CTM) [Allen et al., 1996a, 1996b], using assimilated meteorological data from version 3 of the GEOS data assimilation system [Hou et al., 2004]. The UMD-CTM was run at a resolution of 2° latitude by 2.5° longitude, with 17 sigma layers and 18 pressure layers (35 layers total), a sigma pressure interface of 242 hPa, and a model top pressure of 0.01 hPa. The model forces uniform mixing of CO through the depth of the planetary boundary layer (PBL) at each model time step (15 min). Three-dimensional instantaneous mass concentration of CO is output from the model every six hours.

2.5. Injection Height Scenarios

[31] Five simulations of boreal forest fire smoke injection were performed, each testing an idealized depiction of the injection process. Four of these simulations injected emissions at a single layer in the model, and the fifth distributed emissions in a pressure-weighted scheme throughout the tropospheric column, equivalent to a constant mixing ratio through the column at the emissions source.

[32] In the first case, emissions were inserted at the lowest model layer (BORSFC). They were then mixed instantaneously within the PBL by the CTM, and entrained into the

free troposphere as dictated by the CTM. This scenario enables us to test how well the PBL mixing in the CTM can simulate transfer of forest fire emissions into the free troposphere, without any additional convective uplift.

[33] In the second and third cases, emissions were injected into a layer between 700 and 650 hPa (BOR700) or between 500 and 450 hPa (BOR500). These simulations should depict how emissions are transported that do not spend any time in the PBL prior to entering the free troposphere. In a small fraction of fire events the BOR700 injection layer fell within the PBL.

[34] The fourth case represents rapid uplifting of forest fire emissions through the entire troposphere to near the tropopause (BOR250). Emissions were injected at the top sigma layer in the model (~ 242 hPa).

[35] The final simulation was run using a pressure-weighted distribution of emissions through the tropospheric column (BORMIX). CO mass over the emissions source was distributed proportional to the air mass in each layer, resulting in a constant concentration through the tropospheric column. Given the documented range of injection heights from boreal fires, this simple treatment of injection provides a “null hypothesis” for more sophisticated treatments of smoke injection.

[36] For the remainder of this paper, simulations of CO excluding the boreal fire source will be referred to as BACKGROUND, and simulations including BACKGROUND and BOR sources will be designated as ALL (e.g., BACKGROUND + BORSFC = ALLSFC).

2.6. Observations of CO

2.6.1. Surface Measurements

[37] Surface measurements of CO concentration were obtained from the NOAA Cooperative Air Sampling Network (CASN) (<http://www.esrl.noaa.gov/gmd/ccgg/flask.html>). For this study, flask measurements from all fixed stations were used. The flask samples are intended to represent regional background conditions, and so are generally collected in remote areas. A quality control process is used to flag measurements that are contaminated by local trace gas sources, and flagged measurements were excluded from this study. More information on the measurement, calibration, and quality control of these data can be found in the work of *Novelli et al.* [2003] [see also *Novelli et al.*, 1991, 1998, 1992].

2.6.2. MOPITT Measurements

[38] The MOPITT Level 2 CO product consists of retrieved profiles of CO at up to seven nominal pressure levels, as well as total column CO (TC CO). The MOPITT CO retrieval uses a maximum *a posteriori* optimal estimation technique, which incorporates a contribution from a fixed a priori profile [*Deeter et al.*, 2003]. The instrument takes data over the entire globe every 3 days, with a spatial footprint for each retrieval of 22 km by 22 km. The instrument was operational throughout the study period except for a calibration activity during 4–14 July (<http://www.eos.ucar.edu/mopitt/news/news.html>). The MOPITT CO retrieval is sensitive to cloud cover. Cloud detection at latitudes below 65° is done using MOPITT radiance data, and the MODIS cloud cover product is used at higher latitudes, where clouds are more difficult to resolve in the infrared [*Warner et al.*, 2001]. The MODIS cloud cover

product was unavailable for 6–17 August, and as a result there are no retrievals above 65°N during that period. Only retrievals in the high Northern Hemisphere (HNH, latitude > 30°N) above locations with surface pressures greater than 850 hPa are included in this study.

[39] A number of quality indicators are included with each retrieval, including estimates of the radiometric error and the contribution of the a priori profile to the retrieved profile. The “percent a priori” is reported only for the seven layers of the MOPITT CO profile and not for the total column, so the value for the 700 hPa layer was used to exclude data with greater than 40% contribution of the a priori profile (<1% of data). Retrievals with a radiometric error greater than 25% of the total column CO were also excluded ($\sim 7\%$ of retrievals). These selection criteria resulted in roughly 40,000 usable retrievals in the HNH per full day of instrument operation. A more rigorous filtering of the data produced better agreement with model simulations, but reduced the coverage of the data, especially at high latitudes.

2.7. Resampling of CTM Output for Comparison to CO Observations

2.7.1. Surface CO Measurements

[40] For comparison to CASN surface observations, CTM outputs (6-hourly instantaneous concentration) were sampled in the grid cell containing the measurement location, at the time step nearest the collection date and time for each flask measurement. The resampled CTM output data will be referred to as the CTM-CASN data set in the remaining sections of this paper.

2.7.2. MOPITT CO

[41] Each MOPITT retrieval was matched to its corresponding location on the CTM output grid. A vertical profile of CO concentration was extracted from the CTM output by temporal interpolation of the two time steps nearest the time of the retrieval. This profile was then interpolated to the nominal MOPITT pressure levels. The interpolated profile was then convolved with the a priori profile and the averaging kernel according to the method described by M. N. Deeter, Calculation and Application of MOPITT Averaging Kernels, Natl. Cent. for Atmos. Res., Boulder, Colorado, 2000. (Available at http://mopitt.eos.ucar.edu/mopitt/data/avg_krnls_app.pdf). The result of this calculation is a simulated MOPITT retrieval based on the CTM model output. Total column CO amounts were calculated using the hydrostatic relation, as described by *Emmons et al.* [2004]. Spatial interpolation of these column amounts was used to calculate the total HNH CO burden. The biases and errors associated with each of these processing steps are analyzed in detail in Appendix A. The CTM data sets used for comparison with the MOPITT CO retrievals will be referred to as CTM-MOPITT in the remaining sections of this paper.

2.7.3. Comparison of CTM Output and MOPITT Observations

[42] The application of the averaging kernel and specifically the inclusion of an a priori profile mean that the CTM-MOPITT values are not a simple linear sum of the constituent sources. *Arellano et al.* [2004] describe a method to remove the a priori component of each MOPITT retrieval so that the MOPITT data can be compared to a

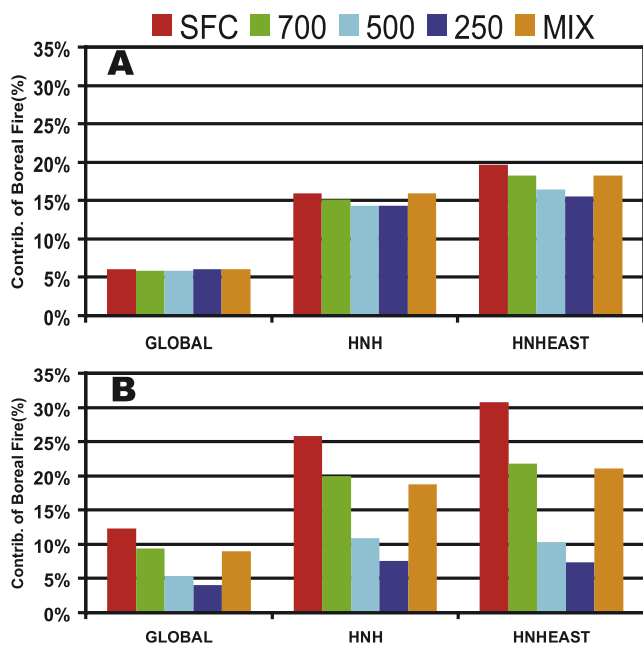


Figure 2. Contribution of boreal forest fire CO in different simulations, as a fraction of (a) total column CO and (b) surface CO concentration. Groups represent different spatial coverage: The leftmost group includes the entire globe, the center group includes only the high Northern Hemisphere (HNH) (above 30°N), and the rightmost group includes only the eastern quadrant (90–180°E) of the HNH.

linear sum of the influence of each constituent in the CTM simulation. This comparison incorporates the averaging kernels and therefore reflects the MOPITT vertical sensitivity, but does not include a contribution from the a priori profile. The disadvantage of this approach is that the values thus obtained cannot be compared directly to observed physical quantities. However, after removal of the a priori component it is possible to consider independently the contributions of different CO source types to the CTM-MOPITT data. Values for individual constituents can also be directly compared to MOPITT observations. For the purposes of this paper, *Arellano et al.*'s [2004] method was used to construct estimates of the boreal fire CO contribution to CTM-MOPITT total column CO. These were compared with the residuals obtained by subtracting the BACKGROUND CTM-MOPITT data from the MOPITT data.

[43] Spatial autocorrelation in the MOPITT data reduces the independence of the sample. Additionally, sampling error caused by the variations in MOPITT sampling density may lead to bias in statistical comparisons. To compare CTM-MOPITT data to MOPITT observations, both simulation and measurement data sets were resampled back onto the 2° latitude by 2.5° longitude by 6 hours CTM output grid. This reduced the sample size but also reduced the sampling bias associated with MOPITT spatial coverage and reduced autocorrelation in the data sets. Resampling also has the effect of partially suppressing the representation error caused by the scale mismatch between MOPITT

observations and CTM output [*Heald et al.*, 2004; *Palmer et al.*, 2003].

3. Results and Discussion

3.1. Effect of Injection Height on Signal From Boreal Fires in CTM Output

[44] The CO concentrations output from the different injection height simulations provide a useful demonstration of the effect of variable injection height on source signal as observed with different types of atmospheric measurements. Here we compare results using different injection scenarios in terms of the differences in distribution of CO, first using the raw model results and then considering what is observable by ground-based and satellite observations using the CTM-CASN and CTM-MOPITT data sets. The relationship between injection height and observed atmospheric signal has important implications for inverse-modeling studies using these atmospheric measurements.

3.1.1. Effect of Injection Height on TC and Surface CO in CTM Simulations

[45] Figure 2 shows the fraction of total simulated CO mass from boreal fires for each injection height scenario, calculated over the entire globe, for just the high Northern Hemisphere, and for the eastern quadrant of the high Northern Hemisphere (90°E–180°E, henceforth “HNHEAST”). Figures 2a and 2b show statistics for total column and surface mean CO, respectively. The sensitivity of model-calculated CO to injection height decreases from the main source region (HNHEAST) to the whole HNH and finally the entire globe.

[46] Differences in global average TC CO between injection scenarios represent the effects of different chemical environments, which are very small overall. Considering only the HNH includes the effects of different meridional transport, which is slightly more efficient for high-altitude sources relative to surface sources. When the analysis is restricted to HNHEAST, zonal transport differences can be seen, which result in much larger differences between scenarios.

[47] The effect of injection height on surface CO is far greater than that on total CO burden. Surface injection of boreal forest fire CO results in a global enhancement of surface CO concentrations more than twice the enhancement produced by high-altitude injection. In the source latitudes, the differences are even greater: boreal forest fire CO injected at the surface contributed 31% to simulated surface CO in the eastern HNH, compared to 8.2% for the same quantity of CO injected near the tropopause.

3.1.2. CTM-CASN Data

[48] Figure 3 is identical to Figure 2b except that surface concentrations were sampled in space and time to match the surface CO observations from the NOAA CASN network. The influence of boreal fires on the global average CO in the CTM-CASN data set is larger compared to unfiltered model output because CASN sampling locations are denser at high latitudes. In the HNH, the contribution of boreal forest fire smoke is underestimated (compare Figure 2b to Figure 3), an effect which is most pronounced near the source region. This reflects the filtering of CASN network observations to

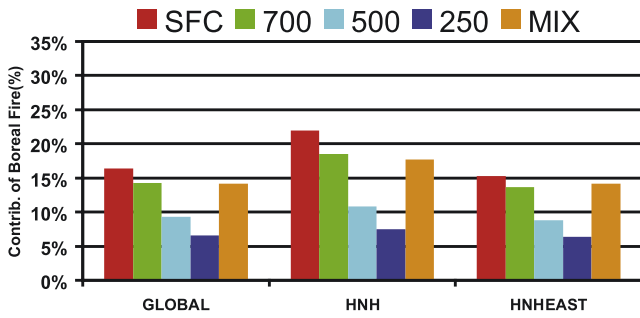


Figure 3. Contribution of boreal source to simulated CO at the locations and times of NOAA Cooperative Air Sampling Network (CASN) observations globally, in the HNH, and in the eastern quadrant of the HNH. Compare to Figure 2b.

remove plumes of unmixed smoke (for detailed analysis of the effects of this filtering on detection of smoke from boreal fires, see Hyer *et al.* [2007]). This simulation shows that the signal from forest fire CO in surface measurements will vary strongly depending on injection height. Despite the filtering of CASN flask data, surface sources produce more than twice the signal in simulated CASN measurements compared with a high-altitude source of the same magnitude.

3.1.3. CTM-MOPITT Data

[49] The MOPITT retrieval derives CO concentration profiles by convolution of MOPITT radiometric observations with an a priori estimate of the vertical profile of CO

in the atmosphere. This means that in retrievals with a strong pollution plume, the response of the MOPITT retrieval will be dependent on the altitude of the plume, as a function of the vertical sensitivity of the MOPITT retrieval. These differences in response must be understood to properly compare model simulations to MOPITT data.

[50] Figure 4 shows the mean vertical profiles of each model run calculated from the raw CTM output (left) and the CTM-MOPITT data set (right). Two effects of the application of averaging kernels to the model output stand out in the comparison between the original CTM output profiles and the CTM-MOPITT profiles. First, all of the single-layer injection simulations show a sharp peak in the mean vertical profile caused by a few profiles close to the emissions source with extremely high CO in the injection layer. Despite being close to the nominal MOPITT retrieval levels, these sharp peaks disappear once the averaging kernel is applied. The other effect is the height-enriched sensitivity of the MOPITT averaging kernel to the upper troposphere and very low sensitivity to the surface. An indication of the sensitivity of the MOPITT instrument is the difference between the ALLSFC and ALL700 simulations in the lower troposphere. In the CTM output, the ALLSFC simulation has much higher CO at the surface. However, once the MOPITT averaging kernel is applied, the ALLSFC CO in the lowest layer of the MOPITT retrieval is lower than the ALL700 CO. This lack of sensitivity at the surface also masks the sharp features in the model output caused by high concentrations in the boundary layer over surface CO sources.

[51] The effects of the vertical sensitivity of the MOPITT retrieval on a transport experiment are illustrated in Figure 5.

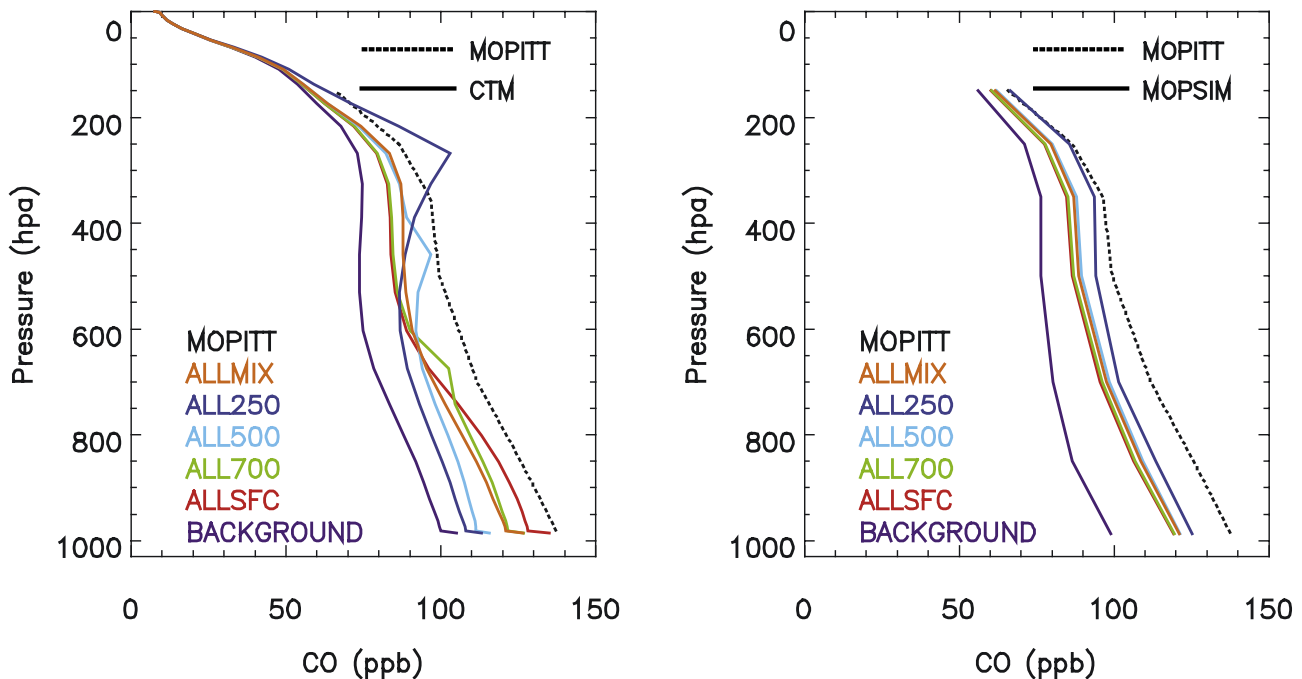


Figure 4. Mean vertical profiles of CO from different injection height simulations. (left) Vertical profiles calculated from the raw 35-level CTM output, after sampling to the locations and times of MOPITT retrievals. (right) Simulated MOPITT vertical profiles resulting from application of the MOPITT averaging kernels to CTM output. MOPITT data are also shown on both graphs (dotted lines).

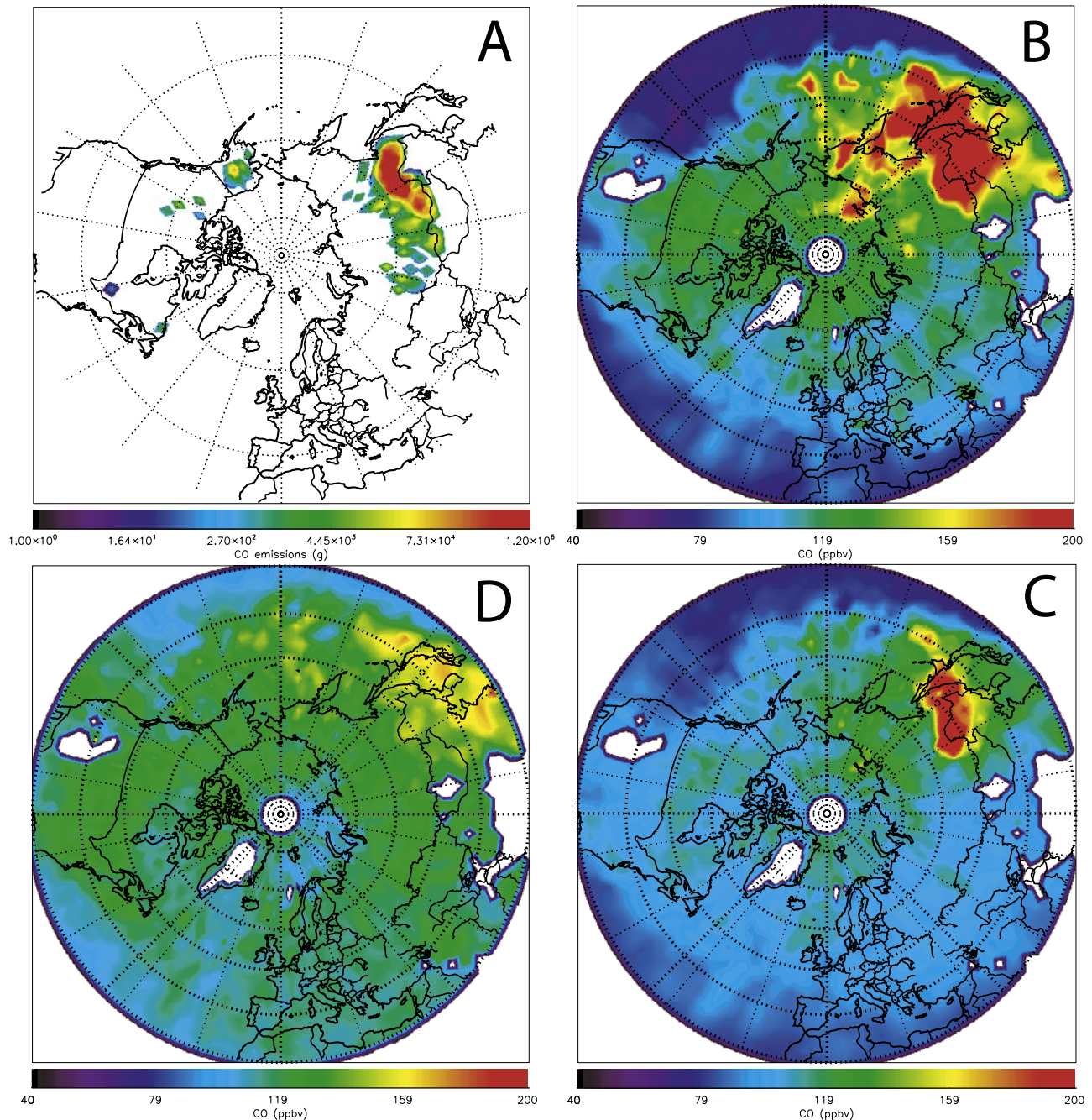


Figure 5. Effect of MOPITT averaging kernels on simulated CO from surface sources in June 2000. (a) Estimated CO emissions from boreal forest fires in June 2000, aggregated to the scale of the CTM. Values are shown in grams, and scale is logarithmic. (b) The 700 hPa CO concentration (in ppbv) from ALLSFC CTM output, sampled to locations of valid MOPITT retrievals. (c) The 700 hPa CO from ALLSFC CTM-MOPITT data (after application of MOPITT averaging kernels). (d) The 700 hPa CO from MOPITT retrievals.

Figure 5a shows the estimated boreal forest fire CO emissions for June 2000, aggregated to the scale of the CTM (2° latitude by 2.5° longitude). Figure 5b shows the mean June CO concentration at 700 hPa, resampled to locations of valid MOPITT retrievals (see section 2.7.2 and Appendix A for details), for the ALLSFC simulation. Figure 5c shows the mean June CO of ALLSFC CTM-MOPITT data, at the nominal 700 hPa level. Figure 5d shows the June mean

700 hPa CO concentration from MOPITT data. Figures 5b and 5c demonstrate how the influence of surface sources (BORSFC in Russia and northern China, as well as fossil fuels and biofuel CO from farther south) is strongly reduced by application of the MOPITT averaging kernel.

[52] This difference in response has strong implications for estimates of the total CO burden in the atmosphere. Figure 6 shows the interaction between injection height and

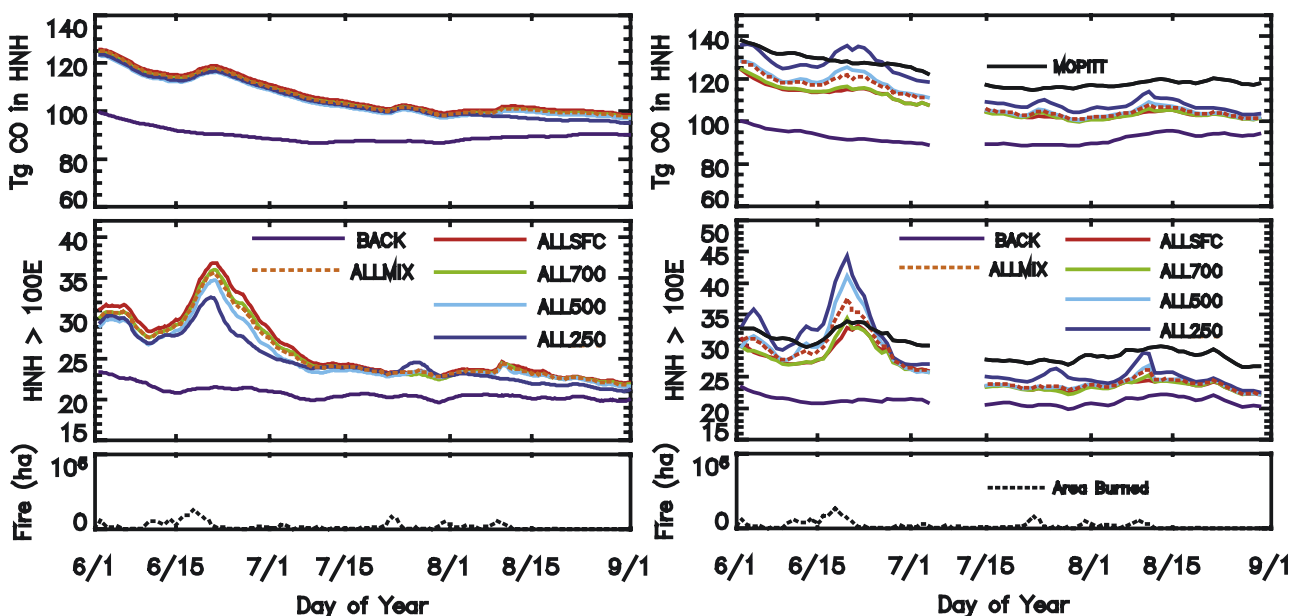


Figure 6. CO burden estimated from CTM outputs for different injection height simulations, integrated over the entire HNH (top) and the eastern quadrant of the HNH (middle). Timing of boreal fire activity is given in the bottom graph. (left) Calculations using the “raw” 35-level output of the CTM; (right) calculations made using the MOPITT sampling and averaging kernel.

the MOPITT averaging kernel. The left-hand graphs show the simulated CO burden from all nonboreal sources and from each of the boreal source simulations, calculated from the raw CTM output (compare to Figure 2a). As noted above, the differences in meridional transport and chemical removal between injection scenarios are quite small. The right-hand graphs in Figure 6 show the same calculation made with CTM-MOPITT total column CO data. CO burden calculated from actual MOPITT observations is also shown for comparison. The lack of sensitivity to variability in CO near the surface results in a dramatically smaller signal from forest fire CO injected at the surface. The high-altitude injection simulation produces an estimated HNH CO burden more than 10% higher than the surface injection simulation, after application of the MOPITT averaging kernel. This comparison demonstrates the sensitivity of MOPITT retrievals to the altitude of CO and ultimately to the source injection height. The differences in CO burden for different injection scenarios have important consequences for attempts to constrain the magnitude of CO sources by inversion of MOPITT data [e.g., Arellano *et al.*, 2004; Petron *et al.*, 2004].

3.2. Comparison of Model Output and Observations

[53] Uncertainty in the magnitude of nonboreal sources makes it difficult to use this experiment to constrain the absolute magnitude of the boreal source. Uncertainty in the spatial and temporal patterns of nonboreal sources can also influence results for the boreal source, and must be considered. In this section, atmospheric observations are first compared with BACKGROUND simulations that do not include any boreal forest fire CO source. Boreal forest fire CO simulations will be evaluated for their skill at capturing residual variability in CO observations, after subtraction of the background simulated CO.

3.2.1. Comparison to NOAA CASN Surface CO Measurements

[54] Table 1 gives statistical results from comparison of the CASN surface CO observations to CTM-CASN model outputs from the BACKGROUND simulation for the three regions used in the comparisons in Figures 2 and 3 (GLOBAL, HNH, and HNHEAST). Figure 7a shows a scatterplot of BACKGROUND CTM-CASN CO versus observations. In Figure 7, observations in the HNH are marked with an asterisk, all other observations are marked with a plus sign. The model captures effectively the contrast between clean air masses (mostly outside of the HNH) and more polluted air masses in the HNH, but is less effective at capturing the variability within the HNH. Correlation between BACKGROUND CTM-CASN data and CASN observations was 0.68 (Pearson’s r) for the entire globe, compared to $r = 0.60$ for the HNH.

Table 1. Statistical Comparison of NOAA CASN Observations to BACKGROUND Simulation With No CO Source From Boreal Fires^a

	Region		
	ALL	HNH	HNHE
N_{obs}	504	282	32
N_{sites}	52	23	4
CASN observed, ppbv, mean	91.7	112.1	159.1
CASN observed, ppbv, σ	38.9	39.9	78.3
CTM-CASN simulated, ppbv, mean	91.8	106.6	120.8
CTM-CASN simulated, ppbv, σ	36.2	38.3	49.6
Bias (observed – simulated), ppbv, mean	0.1	–5.4	–38.3
Bias (observed – simulated), ppbv, σ	29.9	35.1	52.4
RMSE (observed versus simulated), RMSE	29.9	35.5	64.2
Correlation (observed versus simulated), r	0.68	0.6	0.75

^aRegions are as defined in Figure 2. Negative bias values indicate overestimation of CO concentrations by the model. CASN: Cooperative Air Sampling Network.

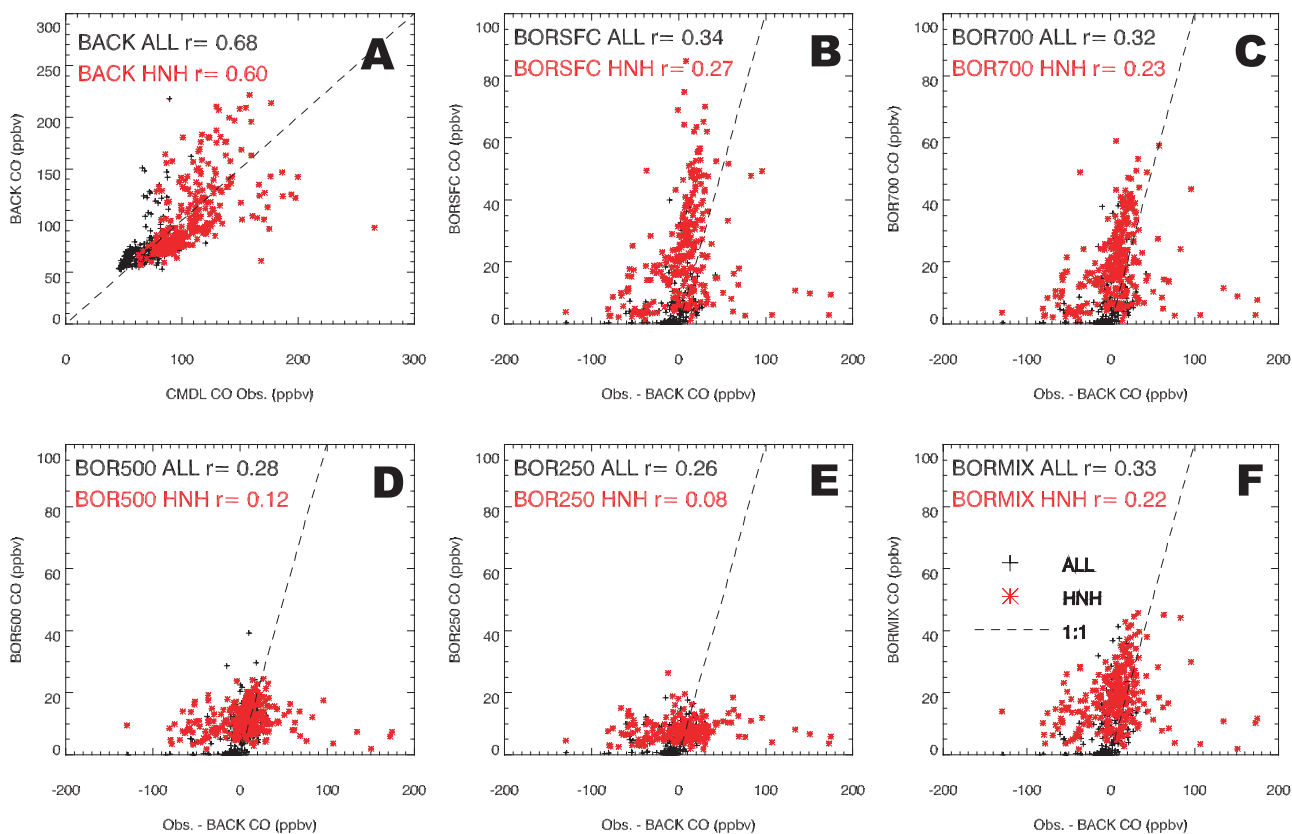


Figure 7. Comparisons of CTM output to surface CO observations from the CMDL Cooperative Air Sampling Network. (a) BACKGROUND simulation compared with CO observations. (b–f) BOR simulations compared with residuals (Observation – BACKGROUND). All CO values are in ppbv. Values for locations in the HNH are indicated with an asterisk, and all other measurements are indicated with plus sign. Dashed line indicates 1:1 relationship.

[55] The HNHEAST region includes only four CASN monitoring stations (Shemya Island, Alaska; Tae-Ahn Peninsula, Korea; Ulaan Uul, Mongolia; and Mt. Waliguan, China), which produced 32 usable measurements during the study period. Comparison of these observations to the BACKGROUND simulation shows CO values were substantially underestimated by the model in this region. This may partly reflect the contribution of boreal forest fire CO, but incorrect specification of other CO source magnitudes is also likely. Numerous studies have identified an underestimate of East Asian CO emissions [e.g., *Hoelzemann et al.*, 2004; *Kasibhatla et al.*, 2002; *Petron et al.*, 2004]. An inverse model experiment by *Palmer et al.* [2003] using data from the TRACE-P campaign found that Asian anthropogenic sources of CO used in this model were potentially underestimated by more than 50%. *Allen et al.* [2004], also using TRACE-P data, showed similar results, finding that the best match to observations was obtained by reducing Asian biomass burning CO by 50% and increasing Asian fossil fuel and biofuel CO by 59%. The TRACE-P measurement campaign took place during March–April 2001, before the onset of the boreal fire season [*Hsu et al.*, 2004]. On the basis of the TRACE-P results, *Streets et al.* [2006] released a revised estimate of Chinese CO emissions 36% higher than the values used in the above studies.

[56] Table 2 gives a statistical comparison of the CO contribution from the modeled boreal source to the residuals obtained by subtracting the BACKGROUND simulation from the surface CO observations. Figures 7b–7f show scatterplots of these data. It is qualitatively clear from the BORSFC comparison (Figure 7b) that model simulation of boreal sources is successful at capturing some of the variability in surface CO measurements not captured by the BACKGROUND sources, though other sources of variability remain. The magnitude of the surface signal decreases with higher injection height: The average CO enhancement from the boreal source is 23 ppbv for the BORSFC simulation, and only 8 ppbv for the BOR250 source. The BOR700 simulation (Figure 7c) shows only slightly less variability at the surface compared to the BORSFC simulation, and is similarly correlated, indicating that CO from 700 hPa is readily mixed down to the surface by the transport model. The BOR500 and BOR250 CO (Figures 7d and 7e) appear to be only rarely mixed to the surface level, and so the CO enhancement from these sources is small and has a smaller range. The contribution of boreal fires is less than 10% of the total BOR250 CTM-CASN CO in over 95% of the data.

[57] The statistics shown in Table 2 indicate that a substantial fraction of the emissions from boreal fires are transported in the surface layer or the lower troposphere

Table 2. Statistical Comparison of CTM Simulations of Boreal Fire CO to NOAA CASN Observations^a

Region	Simulated	Simulated CO Contribution		Bias		RMSE	r
		Mean	σ	Mean	σ		
GLOBAL	BORSFC	15.1	16.2	-15.1	28.7	32.4	0.34
GLOBAL	BOR700	13.1	14	-13.1	28.6	31.5	0.32
GLOBAL	BOR500	8.5	6.5	-8.6	28.8	30.0	0.28
GLOBAL	BOR250	6.1	4.2	-6.1	29.1	29.7	0.26
GLOBAL	BORMIX	13.0	11.4	-13.0	28.3	31.1	0.33
HNH	BORSFC	23.4	16.4	-18.0	34.5	38.9	0.27
HNH	BOR700	19.8	14.2	-14.3	34.6	37.4	0.23
HNH	BOR500	11.6	4.6	-6.1	34.9	35.3	0.12
HNH	BOR250	8.0	3.1	-2.6	35.0	35.0	0.08
HNH	BORMIX	19.0	9.8	-13.5	34.3	36.8	0.22
HNHEAST	BORSFC	18.5	17.4	19.8	55.6	58.2	-0.03
HNHEAST	BOR700	16.5	15.4	21.8	55.5	58.8	-0.06
HNHEAST	BOR500	10.6	5.4	27.7	54.1	60.0	-0.27
HNHEAST	BOR250	7.7	3.6	30.6	52.1	59.7	0.12
HNHEAST	BORMIX	17.1	12.2	21.1	54.2	57.4	-0.03

^aBias is (Observed - [BACKGROUND + BOR]). RMSE and r are calculated by comparing simulation CO contribution from boreal fires to (Observed - BACKGROUND) residuals. All CO values are in ppbv. Negative bias values indicate overestimation of CO concentrations by the model.

(correlation decreases with increasing injection height). However, since surface measurements have very low sensitivity to the BOR500 and BOR250 injection scenarios, the results of this comparison do not indicate what fraction of boreal CO in the troposphere is injected in the middle and upper troposphere. In order to accurately evaluate whether middle and upper tropospheric injection of boreal forest fire smoke contributes to the distribution of CO in the HNH, measurements of CO in the free troposphere must be examined. In the next section, data from the MOPITT instrument are applied to the problem of comparative evaluation of different injection scenarios.

3.2.2. Comparison to MOPITT Observations

[58] MOPITT retrievals in the HNH during the study period were processed according to the method described in section 2.6. The MOPITT analysis used only data from the HNH, and so no global comparisons were made. In addition to the HNH and HNHEAST regions, an additional subset (CONTRAST) was prepared. The CONTRAST subset consists of the 5% of retrievals with the highest variance in CTM-MOPITT TC CO from the different BOR simulations. To determine this subset, CTM-MOPITT TC CO values from each scenario were first normalized to a mean of 0.0 and a standard deviation of 1.0 to account for differences in sensitivity of the MOPITT retrieval. The variance among scenarios of these normalized values was calculated for each retrieval, and the highest 5% taken as the CONTRAST subset. The purpose of creating this subset was to evaluate whether a stronger signal could be obtained by specifically selecting those retrievals where variability among simulations was greatest in the CTM-MOPITT data set.

3.2.2.1. Simulation Without Boreal Fire CO

[59] Table 3 shows statistical estimators of model performance relative to MOPITT, calculated for the subsets described above. All statistics were calculated by comparing the MOPITT total column CO with simulated values from the BACKGROUND simulation. In all regions, the model underestimates CO. The discrepancy between the model and MOPITT data is mostly consistent across geographic

regions, with slightly greater differences in the eastern quadrant of the HNH. Simulated CO is better correlated with observations in the HNHEAST region compared with the entire HNH, which likely reflects better descriptions of the spatial and temporal patterns of Asian emissions (despite problems with the magnitude of these emissions) compared to North American sources [Palmer *et al.*, 2003]. The CONTRAST subset has MOPITT values that are higher and more variable than the HNH as a whole, while BACKGROUND CTM-MOPITT CO has a similar mean and variance in the HNH and CONTRAST subsets. This results in a more negative bias and a larger RMSE for that subset, consistent with a larger contribution from boreal forest fires to those observations.

3.2.2.2. Comparison of Boreal Forest Fire CO in CTM-MOPITT Data to MOPITT Observations

[60] CTM-MOPITT TC CO was compared with MOPITT data to determine which injection scenario corresponded best to the spatial and temporal patterns of CO not captured by the simulated nonboreal sources. Table 4 shows bias, error variance, and model-measurement correlation statistics, comparable to what is shown in Table 2.

[61] The model bias simply reflects the level of observed CO enhancement in each simulation, because the BACKGROUND simulation underestimates the observed CO in all cases. Results from the BACKGROUND simulation above, as well as previous studies using these CO sources [Allen *et al.*, 2004; Heald *et al.*, 2003; Palmer *et al.*, 2003], indicate that much of this underestimate is likely the result of errors in nonboreal CO source magnitudes. Comparison of CO levels in the HNHEAST region to MOPITT observations, shown in Figures 5 and 6, suggests that the boreal CO source is overestimated in this simulation.

[62] The standard deviation of model errors is higher in the HNHEAST region, because of the influence of high CO values near source regions. CTM-MOPITT retrievals from any grid cell containing fire emissions will be elevated, which is a source of representation error because the fire and smoke plume actually occupy only a small fraction of

Table 3. Statistical Comparison of Total Column CO From CTM Simulations Versus MOPITT Observations^a

Region	N _{obs}	MOPITT Observations, molecules cm ⁻² × 10 ⁻¹⁷		BACKGROUND Simulation, molecules cm ⁻² × 10 ⁻¹⁷		Residual, % of MOPITT		RMSE, % of MOPITT	Correlation, r
		Mean	σ	Mean	σ	Mean	σ		
HNH	3,228,289	21.2	3.3	15.9	2.1	25%	13%	28%	0.56
HNHEAST	688,734	22.1	3.9	16.0	2.2	27%	13%	30%	0.69
CONTRAST	161,415	22.9	4.3	15.9	1.7	31%	16%	35%	0.52

^aThe HNH and HNHEAST regions are as used in Figure 2. The CONTRAST region is the 5% subset of maximum variance among the BOR simulations (for details, see section 3.2.2). Positive bias indicates underestimation of CO by the BACKGROUND simulation.

the grid cell, which does not necessarily overlap with any MOPITT retrievals. Thus even when the model is capturing the spatial and temporal variability of the fire source, the scatter of model errors over source regions will be high because of the model's coarse resolution relative to the observations. The strength of the boreal signal in simulated MOPITT total column CO drives the error statistics near the source because of this effect. Thus the scatter in the error is much higher for BOR250 versus BORSFC over Asia and the Pacific, near the source of most of the boreal CO, compared to over North America and the Atlantic.

[63] The additional variance explained by the BOR simulations is modest in all scenarios. The different BOR simulations were all highly correlated, and statistical comparison shows that there is little separation between simulations in terms of agreement with observations. The CONTRAST subset, however, does achieve a better separation of the different simulations. The contribution of boreal fire CO to retrievals in the CONTRAST subset is more than double that for the whole HNH for all injection height scenarios, and the variances of simulation results are also proportionally higher, indicating that the CONTRAST subset should provide a full range of values for evaluating each simulation.

[64] In the CONTRAST subset, and in the data set as a whole, the best agreement with observations was obtained with the BORMIX and BOR500 scenarios. This indicates that if the horizontal and vertical transport in the model are unbiased, the overall vertical distribution of forest fire smoke injection does include some contribution throughout the tropospheric column, and that surface injection may not be a good assumption for broad-scale studies of boreal fire emissions. The correlation of each of the single-layer injection simulations to the MOPITT observations supports this. However, because there are significant covariances among injection simulations, strong conclusions cannot be drawn on the basis of the individual performance of the single-layer scenarios. The resolution of this experiment is not sufficient to specify quantitatively the proportion of emissions injected at the different levels.

4. Conclusions

[65] Boreal forest fires are an important driver of variability in trace gas and aerosol distributions in the high Northern Hemisphere. These fires are often sufficiently energetic to produce convective lofting of emissions. Observations and previous modeling studies have shown that the entrainment of these emissions into the free troposphere

Table 4. Comparison of Simulated Total Column CO From Boreal Forest Fires to MOPITT Observations^a

Region	Simulation	Residuals (MOPITT – BACKGROUND), molecules cm ⁻² × 10 ⁻¹⁷		Simulated Boreal Fire Contribution, molecules cm ⁻² × 10 ⁻¹⁷		Overall Bias, % of MOPITT		Overall RMSE, % of MOPITT	Correlation, r
		Mean	σ	Mean	σ	Mean	σ		
HNH	BORSFC	5.3	2.7	2.8	2.3	11%	13%	17%	0.35
HNH	BOR700	5.3	2.7	2.9	2.7	11%	14%	18%	0.35
HNH	BOR500	5.3	2.7	3.2	3.5	9%	16%	19%	0.38
HNH	BOR250	5.3	2.7	4.1	4.5	5%	21%	21%	0.33
HNH	BORMIX	5.3	2.7	3.2	2.9	10%	14%	17%	0.38
HNHEAST	BORSFC	6.1	2.9	3.4	3.5	12%	16%	20%	0.33
HNHEAST	BOR700	6.1	2.9	3.3	3.8	12%	17%	21%	0.36
HNHEAST	BOR500	6.1	2.9	4.0	5.9	9%	24%	26%	0.40
HNHEAST	BOR250	6.1	2.9	5.0	7.9	4%	34%	34%	0.30
HNHEAST	BORMIX	6.1	2.9	3.8	4.9	10%	21%	23%	0.37
CONTRAST	BORSFC	7.0	3.7	6.9	4.9	0%	24%	24%	0.22
CONTRAST	BOR700	7.0	3.7	7.2	6.3	-1%	28%	28%	0.25
CONTRAST	BOR500	7.0	3.7	8.2	8.5	-6%	35%	36%	0.36
CONTRAST	BOR250	7.0	3.7	9.8	11.5	-13%	49%	51%	0.25
CONTRAST	BORMIX	7.0	3.7	7.8	6.4	-4%	27%	28%	0.33

^a“Residuals” are (MOPITT – BACKGROUND), and “overall bias” is [(MOPITT – (BACKGROUND + BOR))/MOPITT]. In both cases, negative values indicate overestimation of CO by the model. RMSE and r are calculated by comparing simulated CO contribution from boreal fires to residuals. See section 3.2 for details.

Table A1. Statistics of Total Column CO and HNH CO Burden Calculated After Successive Stages of Converting Gridded CTM Output to Simulated MOPITT Retrievals^a

	Raw CTM Output	Resampled to Locations and Times of MOPITT Data	Resampled to MOPITT Nominal Vertical Levels	Averaging Kernel Applied
Total Column CO molecules cm ⁻²				
Mean	1.45×10^{18}	1.51×10^{18}	1.54×10^{18}	1.53×10^{18}
σ	1.74×10^{17}	2.08×10^{17}	2.29×10^{17}	1.90×10^{17}
Bias versus resampled CTM output, % of mean	-	-	3.04×10^{16} (2%)	2.09×10^{16} (2%)
σ of bias	-	-	3.84×10^{16}	1.01×10^{17}
Three-day average HNH CO burden, Tg				
Mean	90.1	90.8	92.4	92.0
σ	2.7	2.7	2.7	2.7
Mean bias versus raw CTM output		0.68	2.29	1.84
σ of bias		0.39	0.49	0.82

^aHNH CO burdens are compared with values calculated from gridded CTM output, while biases in total column CO are calculated by comparison with CTM output resampled to the locations and times of MOPITT retrievals. HNH CO burden statistics exclude the period 6–17 August, when high-latitude MOPITT retrievals were unavailable. For a description of each step, see section 2.7.

can occur at altitudes ranging from 300 m to above the tropopause. We used the UMD global chemical transport model and an early version of the BWEM emissions model to examine how different assumptions about the bulk injection behavior of the boreal forest fire source affected atmospheric simulations, and attempted to evaluate these assumptions using atmospheric measurements from in situ flask measurement data as well as satellite retrievals of CO from the MOPITT instrument.

[66] Our results showed that injection height has important implications for inverse-modeling experiments. The signal in surface CO measurements from boreal fire emissions injected at the surface was more than double that for a source of identical magnitude injected near the tropopause. Conversely, the sampling properties of the MOPITT CO retrieval resulted in estimated total HNH CO burden 10% higher with high-altitude injection of boreal fire CO compared with injection at the surface.

[67] Agreement between transport simulation results with different injection scenarios and atmospheric observations was driven by the vertical sensitivity of the measurements. Surface and near-boundary layer injection produced the best agreement with surface observations, but high-altitude injection scenarios could not be properly evaluated using the surface data because of insufficient variability at the surface. The model results for the five injection height scenarios tested in this study were highly correlated, and comparison to MOPITT measurements over the whole HNH could not achieve much separation to indicate which scenarios were more realistic. However, subsampling of the MOPITT measurements to include only those measurements with a high degree of variance among injection height simulations yielded a much stronger signal. Using this high-contrast subset, we found that pressure-weighted injection through the tropospheric column or injection into the midtroposphere (~500 hPa) produced the best agreement with MOPITT observations.

[68] The next step in description of the bulk properties of the boreal forest fire CO source is to quantify the relative contribution of injection at each level to the atmospheric distribution of CO. The resolution of our experiment was insufficient for this purpose. Accurate description of this

injection process for modeling of atmospheric transport and chemistry is likely to require a physical model capable of capturing variability between fires. The examination of the bulk properties of the source in this study provides a context for finer-scale studies of individual fires. These results also give an indication of the bulk properties one might expect from a broad-scale implementation of a physical plume rise model, such as that used by Freitas *et al.* [2006].

Appendix A: Bias and Error Resulting From MOPITT Sampling Properties Examined Using CTM Output

[69] We performed two tests to describe the effect of transformation of CTM model output (BACKGROUND simulation) to simulated MOPITT data. We calculated total column CO and HNH CO burden from the raw CTM output and at each stage of processing. Results from these tests are shown in Table A1. These statistics do not include the period 6–17 August, when MOPITT retrievals above 65°N are unavailable. CO burden estimates calculated without high-latitude data have a positive bias, because CO concentrations tend to be lower at the poles. Statistics for errors in CO burden were calculated for 3-day averages, reflecting the coverage period of the satellite.

[70] Each column in Table A1 represents a different stage of processing: resampling of the CTM output at the locations and times of MOPITT detections, vertical resampling to the nominal MOPITT retrieval levels, and application of the MOPITT averaging kernels. Bias related to MOPITT spatial and temporal sampling was small (+4%), and mostly related to exclusion of areas of high elevation, which are generally cleaner than the HNH average. Vertical resampling slightly increases the positive bias, because it increases the influence of the surface layer in the TC CO calculation. Application of the averaging kernel has a very small effect on mean bias, but strongly reduces the variance in TC CO.

[71] CO burden results in Table A1 show that if high-latitude data are available, MOPITT can produce depictions of the HNH CO burden at a resolution of 3 days with an accuracy of better than $\pm 4\%$ (95% confidence limit). This result, however, assumes correct specification of the vertical

profile of CO in the atmosphere. Errors will be larger if the altitude of emissions injection is incorrectly simulated. The effect on MOPITT retrievals of sources that release CO into the troposphere at various altitudes is examined in more detail in section 3.1.

[72] **Acknowledgments.** This research was conducted with funding from NASA IDS and a NASA Global Change research fellowship. Preparation of this manuscript was partially funded by ONR code 32.

References

- Allen, D., and K. Pickering (2004), Evaluation of pollutant outflow and CO sources during TRACE-P using model-calculated, aircraft-based, and Measurements of Pollution in the Troposphere (MOPITT)-derived CO concentrations, *J. Geophys. Res.*, *109*, D15S03, doi:10.1029/2003JD004250.
- Allen, D. J., P. Kasibhatla, A. M. Thompson, R. B. Rood, B. G. Doddridge, K. E. Pickering, R. D. Hudson, and S. J. Lin (1996a), Transport-induced interannual variability of carbon monoxide determined using a chemistry and transport model, *J. Geophys. Res.*, *101*, 28,655–28,669.
- Allen, D. J., R. B. Rood, A. M. Thompson, and R. D. Hudson (1996b), Three-dimensional radon 222 calculations using assimilated meteorological data and a convective mixing algorithm, *J. Geophys. Res.*, *101*, 6871–6881.
- Amiro, B. D., J. B. Todd, B. M. Wotton, K. A. Logan, M. D. Flannigan, B. J. Stocks, J. A. Mason, D. L. Martell, and K. G. Hirsch (2001), Direct carbon emissions from Canadian forest fires, 1959–1999, *Can. J. For. Res.*, *31*, 512–525.
- Arellano, A. F., Jr., P. S. Kasibhatla, L. Giglio, G. R. van der Werf, and J. T. Randerson (2004), Top-down estimates of global CO sources using MOPITT measurements, *Geophys. Res. Lett.*, *31*, L01104, doi:10.1029/2003GL018609.
- Bey, I., D. J. Jacob, R. M. Yantosca, J. A. Logan, B. D. Field, A. M. Fiore, Q. B. Li, H. G. Y. Liu, L. J. Mickley, and M. G. Schultz (2001), Global modeling of tropospheric chemistry with assimilated meteorology: Model description and evaluation, *J. Geophys. Res.*, *106*, 23,073–23,095.
- Byram, G. M. (1959), Combustion of Forest Fuels, in *Forest Fire: Control and Use*, edited by K. P. Davis, pp. 61–89, McGraw-Hill, New York.
- Colarco, P. R., M. R. Schoeberl, B. G. Doddridge, L. T. Marufu, O. Torres, and E. J. Welton (2004), Transport of smoke from Canadian forest fires to the surface near Washington, D. C.: Injection height, entrainment, and optical properties, *J. Geophys. Res.*, *109*, D06203, doi:10.1029/2003JD004248.
- Deeter, M. N., et al. (2003), Operational carbon monoxide retrieval algorithm and selected results for the MOPITT instrument, *J. Geophys. Res.*, *108*(D14), 4399, doi:10.1029/2002JD003186.
- Dlugokencky, E. J., L. P. Steele, P. M. Lang, and K. A. Masarie (1994), The growth rate and distribution of atmospheric methane, *J. Geophys. Res.*, *99*, 17,021–17,044.
- Dlugokencky, E. J., B. P. Walter, K. A. Masarie, P. M. Lang, and E. S. Kasischke (2001), Measurements of an anomalous global methane increase during 1998, *Geophys. Res. Lett.*, *28*, 499–502.
- Emmons, L. K., et al. (2004), Validation of Measurements of Pollution in the Troposphere (MOPITT) CO retrievals with aircraft in situ profiles, *J. Geophys. Res.*, *109*, D03309, doi:10.1029/2003JD004101.
- Forster, C., et al. (2001), Transport of boreal forest fire emissions from Canada to Europe, *J. Geophys. Res.*, *106*, 22,887–22,906.
- Freitas, S. R., K. M. Longo, and M. O. Andreae (2006), Impact of including the plume rise of vegetation fires in numerical simulations of associated atmospheric pollutants, *Geophys. Res. Lett.*, *33*, L17808, doi:10.1029/2006GL026608.
- French, N. H. F., E. S. Kasischke, B. J. Stocks, J. P. Mudd, D. L. Martell, and B. S. Lee (2000), Carbon release from fires in the North American boreal forest, in *Fire, Climate Change, and Carbon Cycling in the Boreal Forest*, edited by E. S. Kasischke and B. J. Stocks, Springer, New York.
- Fromm, M. D., and R. Servranckx (2003), Transport of forest fire smoke above the tropopause by supercell convection, *Geophys. Res. Lett.*, *30*(10), 1542, doi:10.1029/2002GL016820.
- Fromm, M., J. Alfred, K. Hoppel, J. Hornstein, R. Bevilacqua, E. Shettle, R. Servranckx, Z. Q. Li, and B. Stocks (2000), Observations of boreal forest fire smoke in the stratosphere by POAM III, SAGE II, and lidar in 1998, *Geophys. Res. Lett.*, *27*, 1407–1410.
- Gerbig, C., J. C. Lin, S. C. Wofsy, B. C. Daube, A. E. Andrews, B. B. Stephens, P. S. Bakwin, and C. A. Grainger (2003), Toward constraining regional-scale fluxes of CO₂ with atmospheric observations over a continent: 2. Analysis of COBRA data using a receptor-oriented framework, *J. Geophys. Res.*, *108*(D24), 4757, doi:10.1029/2003JD003770.
- Giglio, L., J. D. Kendall, and R. Mack (2003), A multi-year active fire dataset for the tropics derived from the TRMM VIRS, *Int. J. Remote Sens.*, *24*, 4505–4525.
- Goode, J. G., R. J. Yokelson, D. E. Ward, R. A. Susott, R. E. Babbitt, M. A. Davies, and W. M. Hao (2000), Measurements of excess O₃, CO₂, CO, CH₄, C₂H₄, C₂H₂, HCN, NO, NH₃, HCOOH, CH₃COOH, HCHO, and CH₃OH in 1997 Alaskan biomass burning plumes by airborne Fourier transform infrared spectroscopy (AFTIR), *J. Geophys. Res.*, *105*, 22,147–22,166.
- Gurney, K. R., et al. (2002), Towards robust regional estimates of CO₂ sources and sinks using atmospheric transport models, *Nature*, *415*, 626–630.
- Heald, C. L., et al. (2003), Asian outflow and trans-Pacific transport of carbon monoxide and ozone pollution: An integrated satellite, aircraft, and model perspective, *J. Geophys. Res.*, *108*(D24), 4804, doi:10.1029/2003JD003507.
- Heald, C. L., D. J. Jacob, D. B. A. Jones, P. I. Palmer, J. A. Logan, D. G. Streets, G. W. Sachse, J. C. Gille, R. N. Hoffman, and T. Nehrkorn (2004), Comparative inverse analysis of satellite (MOPITT) and aircraft (TRACE-P) observations to estimate Asian sources of carbon monoxide, *J. Geophys. Res.*, *109*, D23306, doi:10.1029/2004JD005185.
- Hobbs, P. V., J. S. Reid, J. A. Herring, J. D. Nance, R. E. Weiss, J. L. Ross, D. A. Hegg, R. D. Ottmar, and C. Liouise (1996), Particle and trace gas measurements in the smoke from prescribed burns of forest products in the Pacific Northwest, in *Biomass Burning and Global Change*, edited by J. S. Levine, pp. 697–715, MIT Press, Cambridge, Mass.
- Hoelzemann, J. J., M. G. Schultz, G. P. Brasseur, C. Granier, and M. Simon (2004), Global Wildland Fire Emission Model (GWEM): Evaluating the use of global area burnt satellite data, *J. Geophys. Res.*, *109*, D14S04, doi:10.1029/2003JD003666.
- Hou, A. Y., S. Q. Zhang, and O. Reale (2004), Variational continuous assimilation on TMI and SSM/I rain rates: Impact on GEOS-3 hurricane analyses and forecasts, *Mon. Weather Rev.*, *132*, 2094–2109.
- Hsu, J., M. J. Prather, O. Wild, J. K. Sundet, I. S. A. Isaksen, E. V. Browell, M. A. Avery, and G. W. Sachse (2004), Are the TRACE-P measurements representative of the western Pacific during March 2001?, *J. Geophys. Res.*, *109*, D02314, doi:10.1029/2003JD004002.
- Hyer, E. J., E. S. Kasischke, and D. J. Allen (2007), Effects of source temporal resolution on transport simulations of boreal fire emissions, *J. Geophys. Res.*, *112*, D01302, doi:10.1029/2006JD007234.
- Jost, H. J., et al. (2004), In-situ observations of mid-latitude forest fire plumes deep in the stratosphere, *Geophys. Res. Lett.*, *31*, L11101, doi:10.1029/2003GL019253.
- Kasibhatla, P., A. Arellano, J. A. Logan, P. I. Palmer, and P. Novelli (2002), Top-down estimate of a large source of atmospheric carbon monoxide associated with fuel combustion in Asia, *Geophys. Res. Lett.*, *29*(19), 1900, doi:10.1029/2002GL015581.
- Kasischke, E. S., E. J. Hyer, P. C. Novelli, L. P. Bruhwiler, N. H. F. French, A. I. Sukhinin, J. H. Hewson, and B. J. Stocks (2005), Influences of boreal fire emissions on Northern Hemisphere atmospheric carbon and carbon monoxide, *Global Biogeochem. Cycles*, *19*, GB1012, doi:10.1029/2004GB002300.
- Kuhlbusch, T. A. J., R. G. Zepp, W. L. Miller, and R. A. Burke (1998), Carbon monoxide fluxes of different soil layers in upland Canadian boreal forests, *Tellus, Ser. B.*, *50*, 353–365.
- Lamarque, J. F., et al. (2003), Identification of CO plumes from MOPITT data: Application to the August 2000 Idaho-Montana forest fires, *Geophys. Res. Lett.*, *30*(13), 1688, doi:10.1029/2003GL017503.
- Lavoue, D., C. Liouise, H. Cachier, B. J. Stocks, and J. G. Goldammer (2000), Modeling of carbonaceous particles emitted by boreal and temperate wildfires at northern latitudes, *J. Geophys. Res.*, *105*, 26,871–26,890.
- Leung, F.-Y. T., J. A. Logan, R. Park, E. J. Hyer, E. S. Kasischke, D. Streets, and L. Yurganov (2007), Impacts of enhanced biomass burning in the boreal forests in 1998 on tropospheric chemistry and the sensitivity of model results to the injection height of emissions, *J. Geophys. Res.*, *112*, D10313, doi:10.1029/2006JD008132.
- Livesey, N. J., M. D. Fromm, J. W. Waters, G. L. Manney, M. L. Santee, and W. G. Read (2004), Enhancements in lower stratospheric CH₃CN observed by the upper atmosphere research satellite microwave limb sounder following boreal forest fires, *J. Geophys. Res.*, *109*, D06308, doi:10.1029/2003JD004055.
- Murphy, P. J., J. P. Mudd, B. J. Stocks, E. S. Kasischke, D. Barry, M. E. Alexander, and N. H. F. French (2000), Historical fire records in the North American boreal forest, in *Fire, Climate Change, and Carbon Cycling in the Boreal Forest*, edited by E. S. Kasischke and B. J. Stocks, pp. 274–288, Springer, New York.
- Nelson, R. M. (2003), Power of the fire: A thermodynamic analysis, *Int. J. Wildland Fire*, *12*, 51–65.

- Novelli, P. C., J. W. Elkins, and L. P. Steele (1991), The development and evaluation of a gravimetric reference scale for measurements of atmospheric carbon monoxide, *J. Geophys. Res.*, *96*, 13,109–13,121.
- Novelli, P. C., L. P. Steele, and P. P. Tans (1992), Mixing ratios of carbon monoxide in the troposphere, *J. Geophys. Res.*, *97*, 20,731–20,750.
- Novelli, P. C., K. A. Masarie, and P. M. Lang (1998), Distributions and recent changes of carbon monoxide in the lower troposphere, *J. Geophys. Res.*, *103*, 19,015–19,033.
- Novelli, P. C., K. A. Masarie, P. M. Lang, B. D. Hall, R. C. Myers, and J. W. Elkins (2003), Reanalysis of tropospheric CO trends: Effects of the 1997–1998 wildfires, *J. Geophys. Res.*, *108*(D15), 4464, doi:10.1029/2002JD003031.
- Palmer, P. I., D. J. Jacob, D. B. A. Jones, C. L. Heald, R. M. Yantosca, J. A. Logan, G. W. Sachse, and D. G. Streets (2003), Inverting for emissions of carbon monoxide from Asia using aircraft observations over the western Pacific, *J. Geophys. Res.*, *108*(D21), 8828, doi:10.1029/2003JD003397.
- Petron, G., C. Granier, B. Khatatov, V. Yudin, J. F. Lamarque, L. Emmons, J. Gille, and D. P. Edwards (2004), Monthly CO surface sources inventory based on the 2000–2001 MOPITT satellite data, *Geophys. Res. Lett.*, *31*, L21107, doi:10.1029/2004GL020560.
- Potter, C. S., J. T. Randerson, C. B. Field, P. A. Matson, P. M. Vitousek, H. A. Mooney, and S. A. Klooster (1993), Terrestrial ecosystem production: A process model based on global satellite and surface data, *Global Biogeochem. Cycles*, *7*, 811–842.
- Soja, A. J., W. R. Cofer, H. H. Shugart, A. I. Sukhinin, P. W. Stackhouse Jr., D. J. McRae, and S. G. Conard (2004), Estimating fire emissions and disparities in boreal Siberia (1998–2002), *J. Geophys. Res.*, *109*, D14S06, doi:10.1029/2004JD004570.
- Spichtinger, N., M. Wenig, P. James, T. Wagner, U. Platt, and A. Stohl (2001), Satellite detection of a continental-scale plume of nitrogen oxides from boreal forest fires, *Geophys. Res. Lett.*, *28*, 4579–4582.
- Spivakovsky, C. M., et al. (2000), Three-dimensional climatological distribution of tropospheric OH: Update and evaluation, *J. Geophys. Res.*, *105*, 8931–8980.
- Stocks, B. J., and J. B. Kauffman (1997), Biomass consumption and behavior of wildland fires in boreal, temperate, and tropical ecosystems: Parameters necessary to interpret historic fire regimes and future fire scenarios, in *Sediment Records of Biomass Burning and Global Change*, edited by J. S. Clark et al., pp. 169–188, Springer-Verlag, Berlin.
- Stocks, B. J., et al. (2003), Large Forest Fires in Canada 1959–1997, *J. Geophys. Res.*, *108*(D1), 8149, doi:10.1029/2001JD000484.
- Streets, D. G., et al. (2003), An inventory of gaseous and primary aerosol emissions in Asia in the year 2000, *J. Geophys. Res.*, *108*(D21), 8809, doi:10.1029/2002JD003093.
- Streets, D. G., Q. Zhang, L. T. Wang, K. He, J. Hao, Y. Wu, Y. Tang, and G. R. Carmichael (2006), Revisiting China's CO emissions after the Transport and Chemical Evolution over the Pacific (TRACE-P) mission: Synthesis of inventories, atmospheric modeling, and observations, *J. Geophys. Res.*, *111*, D14306, doi:10.1029/2006JD007118.
- Sukhinin, A. I., et al. (2004), AVHRR-based mapping of fires in Russia: New products for fire management and carbon cycle studies, *Remote Sens. Environ.*, *93*, 546–564.
- Trentmann, J., M. O. Andreae, H. F. Graf, P. V. Hobbs, R. D. Ottmar, and T. Trautmann (2002), Simulation of a biomass-burning plume: Comparison of model results with observations, *J. Geophys. Res.*, *107*(D2), 4013, doi:10.1029/2001JD000410.
- Trentmann, J., G. Luderer, T. Winterrath, M. D. Fromm, R. Servranckx, C. Textor, M. Herzog, H. F. Graf, and M. O. Andreae (2006), Modeling of biomass smoke injection into the lower stratosphere by a large forest fire (Part I): Reference simulation, *Atmos. Chem. Phys.*, *6*, 5247–5260.
- van der Werf, G. R., J. T. Randerson, G. J. Collatz, and L. Giglio (2003), Carbon emissions from fires in tropical and subtropical ecosystems, *Global Change Biol.*, *9*, 547.
- van der Werf, G. R., J. T. Randerson, G. J. Collatz, L. Giglio, P. S. Kasibhatla, A. F. Arellano, S. C. Olsen, and E. S. Kasischke (2004), Continental-scale partitioning of fire emissions during the 1997 to 2001 El Niño/La Niña period, *Science*, *303*, 73–76.
- van der Werf, G. R., J. T. Randerson, L. Giglio, G. J. Collatz, P. S. Kasibhatla, and A. F. Arellano (2006), Interannual variability in global biomass burning emissions from 1997 to 2004, *Atmos. Chem. Phys.*, *6*, 3423–3441.
- Warner, J. X., J. C. Gille, D. P. Edwards, D. C. Ziskin, M. W. Smith, P. L. Bailey, and L. Rokke (2001), Cloud detection and clearing for the Earth Observing System Terra satellite Measurements of Pollution in the Troposphere (MOPITT) experiment, *Appl. Optics*, *40*, 1269–1284.
- Yevich, R., and J. A. Logan (2003), An assessment of biofuel use and burning of agricultural waste in the developing world, *Global Biogeochem. Cycles*, *17*(4), 1095, doi:10.1029/2002GB001952.
- Yurganov, L. N., et al. (2004), A quantitative assessment of the 1998 carbon monoxide emission anomaly in the Northern Hemisphere based on total column and surface concentration measurements, *J. Geophys. Res.*, *109*, D15305, doi:10.1029/2004JD004559.
- Zepp, R. G., W. L. Miller, M. A. Tarr, R. A. Burke, and B. J. Stocks (1997), Soil-atmosphere fluxes of carbon monoxide during early stages of post-fire succession in upland Canadian boreal forests, *J. Geophys. Res.*, *102*, 29,301–29,311.

D. J. Allen, Department of Atmospheric and Oceanic Sciences, University of Maryland, College Park, MD 20742, USA.

E. J. Hyer, Naval Research Laboratory, Marine Meteorology Division, Monterey, CA 93943, USA. (edward.hyer@nrlmry.navy.mil)

E. S. Kasischke, Department of Geography, University of Maryland, College Park, MD 20742, USA.